Protein turnover in the developing *Triticum aestivum* grain

Hui Cao[1] iD **, Owen Duncan[1,2]** iD **and A. Harvey Millar[1,2]** iD

[1]ARC Centre of Excellence in Plant Energy Biology and School of Molecular Science, The University of Western Australia, Bayliss Building M316, Crawley, WA 6009, Australia; [2]Western Australia Proteomics Facility, The University of Western Australia, Bayliss Building M316, Crawley, WA 6009, Australia

Summary

- Protein abundance in cereal grains is determined by the relative rates of protein synthesis and protein degradation during grain development but quantitation of these rates is lacking.
- Through combining *in vivo* stable isotope labelling and in-depth quantitative proteomics, we have measured the turnover of 1400 different types of proteins during wheat grain development.
- We demonstrate that there is a spatiotemporal pattern to protein turnover rates which explain part of the variation in protein abundances that is not attributable to differences in wheat gene expression. We show that *c.* 20% of total grain adenosine triphosphate (ATP) production is used for grain proteome biogenesis and maintenance, and nearly half of this budget is invested exclusively in storage protein synthesis. We calculate that 25% of newly synthesized storage proteins are turned over during grain development rather than stored.
- This approach to measure protein turnover rates at proteome scale reveals how different functional categories of grain proteins accumulate, calculates the costs of protein turnover during wheat grain development and identifies the most and the least stable proteins in the developing wheat grain.

Introduction

Wheat (*Triticum aestivum*) is a trusted source of protein and calories for human consumption and serves as the staple food for 30% of the human population (Shewry & Hey, 2015). Although global wheat production continues to grow steadily, it is not sufficient to meet predicted demand, especially when the global population is projected to exceed nine billion by 2050 requiring an increase of wheat production by about 70% (Tilman *et al.*, 2002; Foley *et al.*, 2011). To cope with such a challenge, researchers, breeders and wheat-processing industries have been working collaboratively to enhance yield while still maintaining grain-quality attributes such as grain protein content (Voss-Fels *et al.*, 2019; Muqaddasi *et al.*, 2020).

While wheat protein content is dominated by glutenin and gliadin storage proteins (Shewry, 2009), it also includes thousands of other components spread through the endosperm, embryo and pericarp (Cao *et al.*, 2016; Duncan *et al.*, 2017). The abundance of high and low molecular weight glutenins determine dough elasticity, while gliadins contribute to dough extensibility (Delcour *et al.*, 2012). A complex pattern of expression of the protein synthesis apparatus and many different types of proteases occur during the early and later stages of grain development (Dominguez & Cejudo, 1996; Nadaud *et al.*, 2010; Rangan *et al.*, 2017). Further, wheat storage proteins are assembled, folded, aggregated and stabilized in the endoplasmic reticulum (ER), and then follow a Golgi or ER route to vacuolar protein bodies (Tosi *et al.*, 2009; Pedrazzini *et al.*, 2016). As a

consequence, the abundance of specific proteins products correlates poorly with expression of the encoding genes in both wheat (Tahir *et al.*, 2020) and many plants (McLoughlin *et al.*, 2018; Reich *et al.*, 2020). Identification and quantification of additional factors that contribute to individual protein abundances and changes in abundance profiles over time are needed to better control wheat grain protein composition.

One such factor is protein turnover rate that dictates how quickly new plant proteins are synthesized while unwanted or dysfunctional proteins are degraded and recycled (Nelson *et al.*, 2014b; Nelson & Millar, 2015; Li *et al.*, 2017). Study of protein turnover rate in plants have focused on either model plants such as Arabidopsis or nonfood tissues of crops, such as seedlings or leaves (Martin *et al.*, 2012; Galland *et al.*, 2014; Nelson *et al.*, 2014a; Yao *et al.*, 2014; Fan *et al.*, 2016; Lyon *et al.*, 2016; Li *et al.*, 2017). These nonfood plant proteomes can be studied in steady-state conditions influenced only by dilution through tissue growth (Nelson & Millar, 2015) and the relatively short lag period for introduction of stable isotopes makes calculating protein turnover measurements in these systems feasible (Nelson *et al.*, 2014a; Li *et al.*, 2017). In comparison, studying grain filling is complicated by the complex dynamics of protein accumulation during development and the relative difficulty of rapidly introducing stable isotopes into the spike (Dawson *et al.*, 2002).

Here, we have overcome these technical and biological challenges to establish *in vivo* stable isotope (nitrogen-15, ^{15}N) labelling to enable protein turnover rates to be measured during wheat grain development. Using this approach, we monitored

synthesis and degradation rate of over 1400 different wheat protein types during grain filling and calculated the adenosine triphosphate (ATP) energy usage for protein synthesis and degradation. Wheat grain protein turnover rates provide scientists and breeders with a quantitative and in-depth understanding of how each wheat grain protein accumulates and a biotechnological pathway to craft a lower cost grain proteome.

Materials and Methods

Plant materials and growth condition

Wheat (*Triticum aestivum* L.) plants of cv Wyalkatchem, were grown in an indoor chamber under 16 h : 8 h, light : dark conditions with 26°C : 18°C, 60% humidity and light intensity of 800 µmol $m^{-2} s^{-1}$. The hydroponic growth system used for plant growth is described by Munns & James (2003). Briefly, 50 l of Hoagland solution was used for 24 plants and changed weekly (Duncan *et al.*, 2017). Seeds were vernalized under 4°C for 3 d before being transferred to the growth chamber followed by 3–5 d germination until two leaves emerged at which point they were transferred to the hydroponic growth system. Plants were firstly grown with natural abundance N medium, which was then replaced with ^{15}N (^{15}NH$_4$^{15}NO$_3$, 98%, Sigma fine chemicals; Sigma) medium for a labelling programme when plants reached the required growth stage (e.g. 7 d post-anthesis, 7 DPA). Plant roots were rinsed three times with distilled deionized water before being transferred to the ^{15}N medium. A set of fully labelled plants to generate the spike-in standard samples were grown with ^{15}N medium at all times after germination. Grain samples, including unlabelled, progressive labelled and fully labelled samples, were harvested at multiple time points as shown in Supporting Information Figs S1 and S2. Only eight grains from the middle of the ear (both floret 1 and 2) were collected in each case. Grain tissues of embryo, endosperm and pericarp were hand-dissected by scalpel. Due to the challenge of separating embryo from endosperm in young grain, only 14 and 17 DPA-old grain were used for dissection and tissue samples of two time points were pooled together. Samples were snap frozen in liquid nitrogen (N$_2$) and stored in − 80°C for further protein extraction.

Grain respiratory oxygen consumption rate measurement

Respiration rates of single premature grain at different growth age (7, 10, 14, and 17 DPA) were measured using a Q2 oxygen sensor (Astec-Global, Maarssen, the Netherlands) in sealed 2 ml capacity tubes at 24°C. The oxygen (O$_2$) concentration within tubes were measured at an interval of 5 min for 16 h. In total, 64 replicates, including eight biological replicates (from different plant) with eight technical replicates (eight grains from the same ear), were performed for each growth stage. The O$_2$ consumption rate (R_N) trace was generated using a moving slope of O$_2$ consumption in a 2 h window and the formula reported by Scafaro *et al.* (2017). The representative R_N was calculated using the O$_2$ consumption slope in the 2 h window from 1 to 3 h. Total ATP production of a single wheat grain at each growth stage was also

estimated based on the ATP production rates of 1 O$_2$ to 4.5 ATP (Li *et al.*, 2017).

Spike-in approach for individual wheat grain fold changes in protein abundance measurement

To precisely measure individual fold changes in protein abundance (FCP) of wheat grain proteins during grain development, a spike-in approach was developed to avoid changes in protein : starch ratio impacting our calculations. Briefly, an equal number of ^{15}N fully labelled grains (eight grains in this study) of each time points (7, 10, 14 and 17 DPA) were pooled together and ground using mortar and pestle under liquid N$_2$. A 100 mg fresh weight aliquot of this fully labelled fine ground powder, as an internal standard, was spiked into four unlabelled grains from each time point of grain development followed by another grinding (Fig. S2b). These spike-in containing samples were store in − 80°C for subsequent protein extraction, mass spectrometry (MS) data acquisition and FCP measurement.

Sample preparation

A chloroform/methanol extraction protocol (Wessel & Flugge, 1984) was applied for total protein extraction in this study. Briefly, 200 mg sample powder generated by extensive grinding in liquid N$_2$ was mixed with 400 µl extraction buffer (125 mM Tris–HCl pH 7.5, 7% (w/v) sodium dodecyl sulphate (SDS), 0.5% (w/v) PVP40, Roche protease inhibitor cocktail (Roche, one tablet per 50 ml)) and rocked on ice for 10 min. After a centrifugation at 10 000 *g* for 5 min, about 200 µl supernatant was transferred into a new 2 ml Eppendorf tube, followed by protein precipitation through mixing the supernatant with 800 µl methanol, 200 µl chloroform and 500 µl distilled deionized water. The pellet was washed twice using methanol and then incubated with 90% (v/v) acetone at −20°C twice for at least 1 h each time. After drying at room temperature, protein pellet was resuspended using resuspension buffer (50 mM Ambic, 1% (w/v) SDS and 10 mM DTT). Protein concentration was quantified by an amido black method (Schaffner & Weissmann, 1973).

Proteins (200 µg) were incubated with 20 mM DL-dithiothreitol for 20 min in darkness at room temperature, followed by a second incubation with 25 mM iodoacetamide for 30 min in darkness at room temperature. After diluting the SDS to its working concentration at 0.1% (w/v) via adding distilled deionized water, proteins were digested overnight using trypsin (sequencing grade modified trypsin; Promega) at 37°C with protein : trypsin ratio of 50 : 1. The SDS removal and high-pH, reversed phase peptide fractionation for digested peptide solution (Wang *et al.*, 2011) were conducted on off-line high-performance liquid chromatography (HPLC) (1200 series; Agilent Technologies, Santa Clara, CA, USA) combining with two J4SDS-2 guard columns (PolyLC) and an XBridge™ C18 3.5 µm, 436 mm × 250 mm column (Waters, Milford, MA, USA). The pump flow was set at 0.5 ml min^{-1} using the following solution B (90% acetonitrile with 10 mM ammonium formate (pH 10/NH$_4$OH)) gradient: 2–5% in 6 min, 5–35% in

60 min, 35–70% in 13 min, 70–100% in 10 min and 100 to 2% in 3 min. In total, 64 fractions for each sample were collected from 15 to 79 min in 1 min windows. The first 12 and last 4 fractions (low peptide abundance and detergent contaminated fractions) were discarded and the rest of the fractions in the same column of the 96 well plate were combined together. The final 12 fractions of each sample were dried down through a vacuum centrifuge and store in −80°C for further MS analysis.

Liquid chromatography–mass spectrometry data acquisition

Peptide fractions were resuspended with 25 µl of 5% (v/v) acetonitrile and 0.1% (v/v) formic acid in HPLC grade water followed by a filtering step using 0.22 µm centrifugal filters (Millipore). Purified peptide suspensions (2 µl each) were injected into a HPLC-chip (Polaris-HR-Chip-3C18; Agilent Technologies) through a capillary pump with a flow at 1.5 µl min^{-1}. Peptides were eluted from the C18 column online into an Agilent 6550 Q-TOF. Gradients were generated by a 1200 series nano pump (Agilent Technologies) with the nano flow at 300 nl min^{-1}, of which 5–35% (v/v) solution B (0.1% (v/v) formic acid in acetonitrile) in 35 min, 35–95% in 2 min and 95–5% in 1 min. Parameters setting in MS acquisition was as described previously (Duncan *et al.*, 2017). In total, liquid chromatography–mass spectrometry (LC–MS) data of 516 fractions were successfully collected (Fig. S2d). The primary MS data files are available via ProteomeXchange with identifier PXD022231. Details of LC–MS data processing to generate FCP, labelled protein fraction (LPF), protein turnover and ATP costs are provided in Methods S1.

Gas chromatography–mass spectrometry data acquisition and processing

Grain sample powder of 30 mg were mixed with 250 µl metabolite extraction buffer (85% (v/v) methanol, 15% (v/v) distilled deionized water, and 0.1 mol l^{-1} sorbitol (D-sorbitol-$^{13}C_6$) as the internal standard), and subsequently incubated on a thermomixer at 75°C and 950 rpm for 10 min. After mixing with 125 µl of chloroform and 250 µl of distilled deionized water, sample solutions were centrifuged for 15 min at 2000 *g*, of which 50 µl of supernatant was transferred to a new tube and dried out using a vacuum centrifuge. Sample derivatization started with an incubation in 20 µl of 20 mg ml^{-1} methoxyamine hydrochloride in pyridine for 2 h at 37°C, followed by a second incubation in 20 µl of *N*-methyl-*N*-(trimethylsilyl)-trifluoroacetamide (Sigma) for 30 min at 37°C. Incubations were conducted on a thermomixer at 950 rpm. Volume of 40 µl derivatized sample was transferred to glass vials for gas chromatography–mass spectrometry (GC–MS) analysis. Metabolites samples of 1 µl were injected into an Agilent 7890A gas chromatograph coupled with a Varian CP9013-Factor 4 column (40 m, 30.25 mm inner diameter (i.d.)) and an Agilent 5975 quadrupole mass spectrum detector. GC–MS data acquisition was performed following descriptions reported by O'Leary *et al.* (2017). GC–MS data were processed

and analysed using Agilent MassHunter Workstation (v.10.1) as mentioned earlier.

Gene expression data retrieval

Gene expression data of the key storage proteins were downloaded from the Wheat Expression Browser website (http://www.wheat-expression.com/) (Borrill *et al.*, 2016; Ramirez-Gonzalez *et al.*, 2018). Only Chinese Spring grain tissue data at 2, 14 and 30 DPA under nonstress conditions (choulet_URGI) were used in this study.

Statistical analysis

Data processing, statistical analysis and visualization were performed in the R environment (v.3.5.1). Statistical tests and replicate number are as shown in figure and figure legends.

Results

In vivo stable-isotope nitrogen (^{15}N) labelling of wheat grain proteins

Measuring the synthesis and degradation of individual wheat proteins requires the labelling of new proteins in grains. We undertook this labelling by incorporation of the stable isotope ^{15}N into the amino acids used for their synthesis (Nelson *et al.*, 2014b; Nelson & Millar, 2015). Wheat grain development includes cell division and expansion until 14 DPA, grain filling (14–28 DPA), and desiccation and maturation (28–42 DPA) (Rogers & Quatrano, 1983). To determine when during development the turnover rate of wheat grain proteins could be measured, four sets of wheat plants were raised in hydroponic medium with N salts of natural isotope abundance (99.6% ^{14}N, 0.4% ^{15}N) until plants reached 7, 14, 21 and 28 DPA, respectively. The growth media of natural N isotopes was then replaced by heavy ^{15}N labelled media (2% ^{14}N, 98% ^{15}N). Grain samples were harvested after 7 d of continuous labelling (Fig. S1a). Peptide MS analysis showed that nearly 25% of N atoms in newly synthesized proteins in wheat grain were ^{15}N after the 7-d labelling period, regardless of the grain DPA (Fig. S1b). Broadly, calculations of the labelled protein fraction can be made independently of the percentage of ^{15}N they contain, making this technique robust to differences in ^{15}N incorporation rate (Nelson *et al.*, 2014b; Li *et al.*, 2017). We found younger grains showed a higher proportion of newly synthesized proteins in their total protein pool (LPF) than older grains (Fig. S1c). However, we know that at least 20% of ^{15}N incorporation is required to make high-quality protein turnover rates measurements with false discovery rate (FDR) < 1% (Nelson *et al.*, 2014a), we worked to achieve this basal rate by focusing on 7 DPA-old grain as our first time point for subsequent labelling experiments. To capture the major events of grain development, samples of progressively labelled grain were collected after 3, 7 and 10 d of continuous ^{15}N labelling to span the 7 DPA to 17 DPA period (Fig. S2a). A significant expansion was seen in grain size over this time period

with single grain fresh weight tripling over 10 d from 25 mg at 7 DPA to 78 mg at 17 DPA (Fig. 1a,b; Table S1). The ^{15}N enrichment level gradually increased over time from 20% after 3 d (10 DPA) to 29% after 10 d (17 DPA) (Fig. 1c; Table S1).

One day lag time in labelling of wheat grain proteins

Incorporation of nitrogen into the developing grain requires long-distance transport from the roots through the phloem, before its assimilation, use and storage in leaves and the spike (Fischer *et al.*, 1998). Using a logarithmic regression model and our 3, 7 and 10 d labelling data, we calculated a lag of 28 h (Fig. S3a; Table S2). To confirm this lag time estimated, we used both GC–MS analysis of free amino acids and LC–MS analysis of peptides to assess the ratio of heavy (+ 1) to mono abundance of amino acids and peptides in samples collected in the first 30 h of labelling. We found both amino acids and peptides of proteins remained at their natural abundance level before 24 h but rapidly rose between 24 and 30 h following ^{15}N labelling (Figs S3b,c, S4; Table S2).

Grain respiration rate and adenosine triphosphate production

Protein production is a major user of cytosolic ATP generated through oxidative phosphorylation. Using a fluorophore-based oxygen sensor, we measured the grain respiration rate during grain development and found younger grains respired at twice the rate of older ones on a fresh weight basis (Fig. 1d; Table S1). As cellular respiration is the primary ATP production source in

wheat grain, and assuming a cellular ATP production ratio of 1 O_2 to 4.5 ATP (Li *et al.*, 2017), the total ATP production rate of a single grain was calculated to be 37, 60, 54 and 54 µmol ATP per day for grains at 7, 10, 14 and 17 DPA, respectively (Table S1).

Calculating individual fold changes in protein abundance for proteins during wheat grain development

As the proteome of the wheat grain is not in a steady-state during filling, we needed to obtain individual FCP values for each protein of the wheat grain. To do this a spike-in procedure was developed that involved adding a standard amount of a fully ^{15}N labelled wheat grain standard (see Materials and Methods section) to four grains from each time point. This helps to define proteins rapidly accumulating in the grain and exclude the effect of differential starch accumulation on the measurements (Fig. S2b). Using this approach, quantification of the abundance change of 2307 nonredundant grain proteins were measured using data from over 71 000 independently quantified peptides. Principal component analysis (PCA) of the quantitative data set showed that grain samples separated according to their DPA with the first principal component explaining nearly 94% of the variation. Only minor variation was observed in the second principal component and biological replicate samples of the same time point were closely clustered together (Fig. S5a; Table S3). Over half of the identified proteins increased in abundance ≥ 2-fold from 7 DPA to 17 DPA, with a few exceptions that showed the opposite pattern, consistent with net protein accumulation during grain development (Fig. 2a; Table S4a). Quantitative
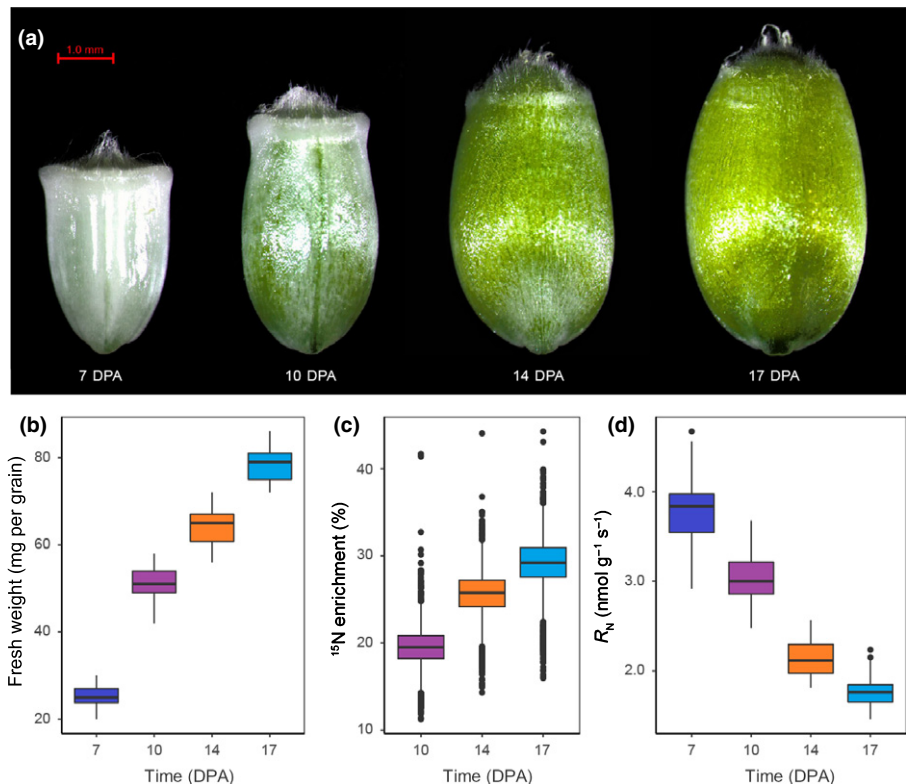

Fig. 1 Time-dependent changes in grain size, fresh weight, respiration rate and nitrogen-15 (^{15}N) labelling of newly synthesized protein. (a) A representative image of wheat grain at different developmental stages. (b) The fresh weight of individual grain at different developmental stages (*n* = 64). (c) The ^{15}N enrichment in newly synthesized proteins at 10, 14 and 17 d post-anthesis (DPA) after a switch to ^{15}N media at 7 DPA. (d) Respiration rate (R_N) of wheat grain at different developmental stages expressed as oxygen (O_2) consumption rate (nmol O_2 per gram fresh weight per second; *n* = 64). Thick horizonal bars in the boxes indicate median values, box limits are upper and lower quartiles, whiskers represent 1.5 interquartile ranges, and dots represent outliers. Detailed data used in this analysis are listed in Supporting Information Table S1.
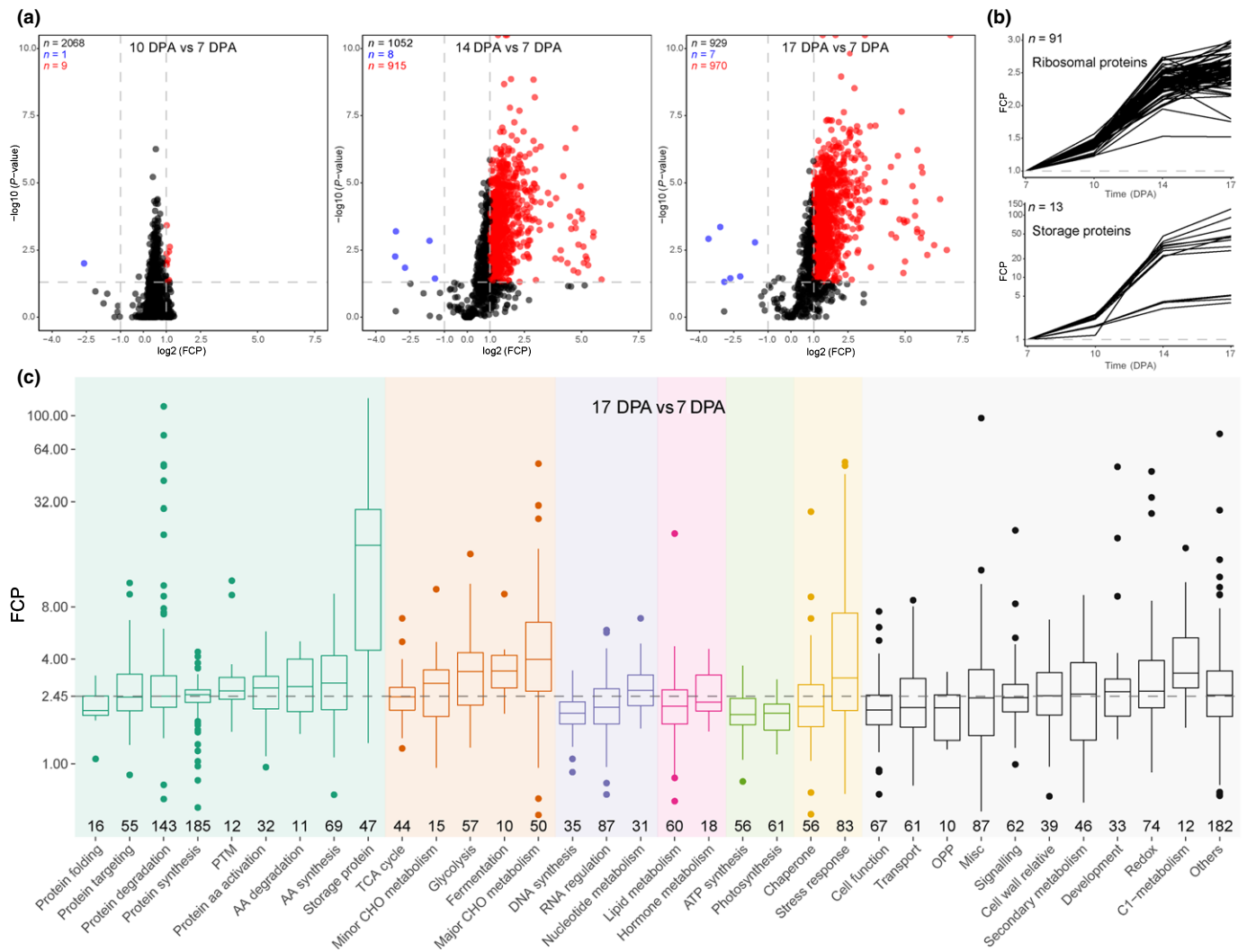
Fig. 2 Fold changes in protein abundance (FCP) of 2307 proteins during wheat grain development. (a) Volcano plots of all FCP at each time point. Proteins with a fold change in abundance ≥ 2 or ≤ 0.5 and with a P-value ≤ 0.05 are shown by red circles (increase abundance) or blue circles (decrease abundance), respectively. All other data points are shown as black circles. The number of proteins of each colour is shown on the top-left corner of each plot, and dashed lines indicate the cut-off value of FCP and P-value. (b) Examples of slow FCP of ribosomal proteins compared to the rapid accumulation of storage proteins during grain development. (c) Proteins with fold change in abundance between 7 d post-anthesis (DPA) and 17 DPA are shown in 34 functional categories (≥ 10 proteins) within seven broad functional categories. Proteins in all other categories (≤ 10 proteins per category) are grouped into the 'Others' category. The number of proteins in each category is displayed along with x-axis, and functional categories were sorted within each super category by increasing median FCP. The y-axis is $\log_2$ transformed FCP and the dashed line shows the overall median FCP across all wheat grain proteins. Thick horizonal bars in the boxes indicate median values, box limits are upper and lower quartiles, whiskers represent 1.5 interquartile ranges, and dots represent outliers. Pairwise t-test results between categories are listed in Supporting Information Table S4. Broad functional categories are: amino acid metabolism (green), carbohydrate metabolism (orange-red), nucleotide metabolism (purple), lipid metabolism (pink), energy producing (lawngreen), stress response (gold) and 'Other' categories (black).

abundance changes for different proteins during grain development varied from 0.018-fold to 126-fold. Examples shown in Fig. 2(b) illustrate the dynamics of different protein groups such as ribosomal proteins (fold change < 3 over 10 d) and storage proteins (fold change > 25 on average and up to 126 over 10 d).

MapMan functional category bins (Thimm *et al.*, 2004) were used to separate identified proteins into 34 groups (≥ 10 proteins in each). These showed a median fold change value of 1.38-, 2.31- and 2.45-fold change at 10, 14 and 17 DPA compared to 7 DPA (Figs 2c, S6). Exceptions were found in the categories of storage proteins, major CHO metabolism and stress response,

where fold change values significantly higher than the median were observed. These data are consistent with biogenesis and accumulation of starch and storage proteins being major events during grain development and moisture loss in ripening and maturation being a post-anthesis stress (Blum *et al.*, 1983). Protein categories associated with protein folding, tricarboxylic acid (TCA) cycle, DNA synthesis and photosynthesis showed lower fold change than the median, likely because they were less active cellular pathways during grain development. Together this evidence showed clear temporal patterns in the regulation of protein abundance during grain development.

Calculating wheat grain protein synthesis and degradation rates during grain development

The LPF is an instantaneous measurement of the ratio between existing and new protein molecules for each individual proteins of interest at a given point of time. This information is derived from the ratio of peptides for a protein with greater than natural abundance (labelled) to the sum of peptides with natural abundance and greater than natural abundance ($^{15}N/(^{14}N + ^{15}N)$)). These measurements are derived from quantitation of the deviation of the isotopic envelope from what would be expected of natural abundance peptides of a particular sequence (Nelson *et al.*, 2013; Li *et al.*, 2017). LC–MS/MS results from 252 fractionated samples, including 108 fractions of progressive labelling samples and 144 fractions of unlabelled samples, provided data on over 44 000 quantified peptides. Combining the information from peptides derived from the same protein allowed us to measure the LPF of 1711 nonredundant proteins from wheat grains. The median of the relative standard deviation from the mean (RSD) for each protein at a given time point was less than 11% across all three time points (Table S5). Spearman correlation coefficient analysis showed a relatively high correlation of LPF between biological replicates ranging from 0.81 to 0.95 (Fig. S5g; Table S3). PCA suggested that up to 97% of the variation observed could be explained by the first principal component alone (Fig. S5d; Table S3). Through combining the individual FCP and LPF values for specific proteins, we then calculated protein synthesis rates and degradation rates for 1447 nonredundant proteins (Table S5). Relative protein synthesis rates (K_S/A; where K_S is the synthesis rate constant and A the abundance of protein) varied nearly 100 fold; ranging from 0.057 to 5.27 d^{-1} with a median of 0.35 d^{-1}. By contrast, protein degradation rates (K_D; where K_D is the degradation rate constant) had a median of 0.11 d^{-1} and ranged from effectively zero up to 0.94 d^{-1}. The latter indicates a range of proteins in grain with half-lives of less than 1 d.

To determine if subcellular location influenced protein turnover rates in wheat grain, we grouped the data set by their subcellular location retrieved from a database of crop proteins with annotated locations (cropPAL) (Hooper *et al.*, 2016). We reassigned storage proteins into vacuole because once assembled in ER, storage proteins are transported to protein storage vacuoles (PSVs) (Herman & Larkins, 1999). Based on this, vacuole proteins, predominantly storage proteins, showed higher median synthesis and degradation rates than other subcellular structures. The same pattern was found in subcellular protein sets of the peroxisome, Golgi apparatus and extracellular secreted proteins (Et), but the opposite pattern was seen in protein sets located in the mitochondrion, cytosol, plastid and the ER (Fig. 3a). These observations generally agreed with published data from Arabidopsis leaves which showed organellar proteins that are physically separated from the cytosolic proteolysis system have relatively lower degradation rate, while cellular structures such as the Golgi apparatus have a frequently updated protein complement and a relatively higher turnover rate (Li *et al.*, 2017).

When the data were arranged by MapMan functional category bins, most of the 37 major groups maintained a median K_S/A of 0.35 ± 0.15 d^{-1} and median K_D of 0.11 ± 0.05 d^{-1} (Fig. 3b). However, exceptions were found, notably stable photosynthesis proteins had a median K_S/A of 0.24 d^{-1} and median K_D of only 0.03 d^{-1}, while storage proteins had a median K_S/A of 2.17 d^{-1} and median K_D of 0.48 d^{-1}, indicating rapid synthesis and degradation cycling of a portion of storage proteins in developing grains. Variation of protein turnover rates was also observed for proteins located in the same organelle or subcellular structure but which belonged to different functional categories, or vice versa, such as cytosolic proteins involved in ATP synthesis, protein folding and protein synthesis, or RNA regulation factors located in the cytosol and nucleus (Fig. 3b). To better understand the connection between protein functional roles and their turnover rates, we compared turnover rate profiles between three sets of rapidly-cycling proteins and three more stable house-keeping protein sets. The K_S/A of the rapidly-cycling proteins gradually increased or stayed steady over development, while a much lower synthesis rate and decreasing K_S/A over development was observed for more stable house-keeping functional categories (Fig. 3c). As expected, much lower K_D was determined for house-keeping proteins in comparison with rapidly-cycling proteins, but unlike protein synthesis rate, both protein types shared a similar pattern over development, notably that K_D dropped from its peak at 10 DPA to its lowest level at 14 DPA followed by a slight increase by 17 DPA.

Storage proteins were prominent members of lists of the 20 most rapidly synthesized proteins (55%) and the 20 most rapidly degraded proteins (30%) in wheat grains; this included gliadins, globulins, high-molecular-weight glutenin subunits (HMW-GS) and low-molecular-weight glutenin subunits (LMW-GS) (Table S5). Proteins annotated as responding to stress conditions were the second most numerous in both lists; four were on the 20 most rapidly synthesized list and three were on the most rapidly degraded list. An alpha-amylase inhibitor (TraesCS6D01 G000200.1) topped the degradation rate list and had a calculated half-life of only 0.74 d^{-1}.

To facilitate further comparisons, we used filters to select a set of 149 wheat proteins that were synthesized rapidly ($K_S/A \geq 2 \times$ median K_S/A of 0.71 d^{-1}) and a set of 67 proteins that were synthesized slowly ($K_S/A \leq 0.5 \times$ median K_S/A of 0.18 d^{-1}). These two groups represented roughly 10% and 5% of all measured proteins, respectively (Table S5). Adopting the same filtering principles, 291 (*c.* 20%) and 320 (*c.* 22%) proteins were selected as rapidly and slowly degrading proteins, respectively. These groups were then further clustered as being house-keeping proteins (i.e. both slow K_S/A and K_D, SS), induced but stable proteins (i.e. fast K_S/A and slow K_D, FS), and rapidly-cycling proteins (i.e. both fast K_S/A and K_D, FF) (Fig. S7a). Functional category analysis of these sets showed that the house-keeping proteins mainly participated in photosynthesis, DNA synthesis and glycolysis; while induced but stable proteins participated in major CHO metabolism, transport and amino acid synthesis proteins; and the rapidly-cycling protein set was dominated by storage proteins,
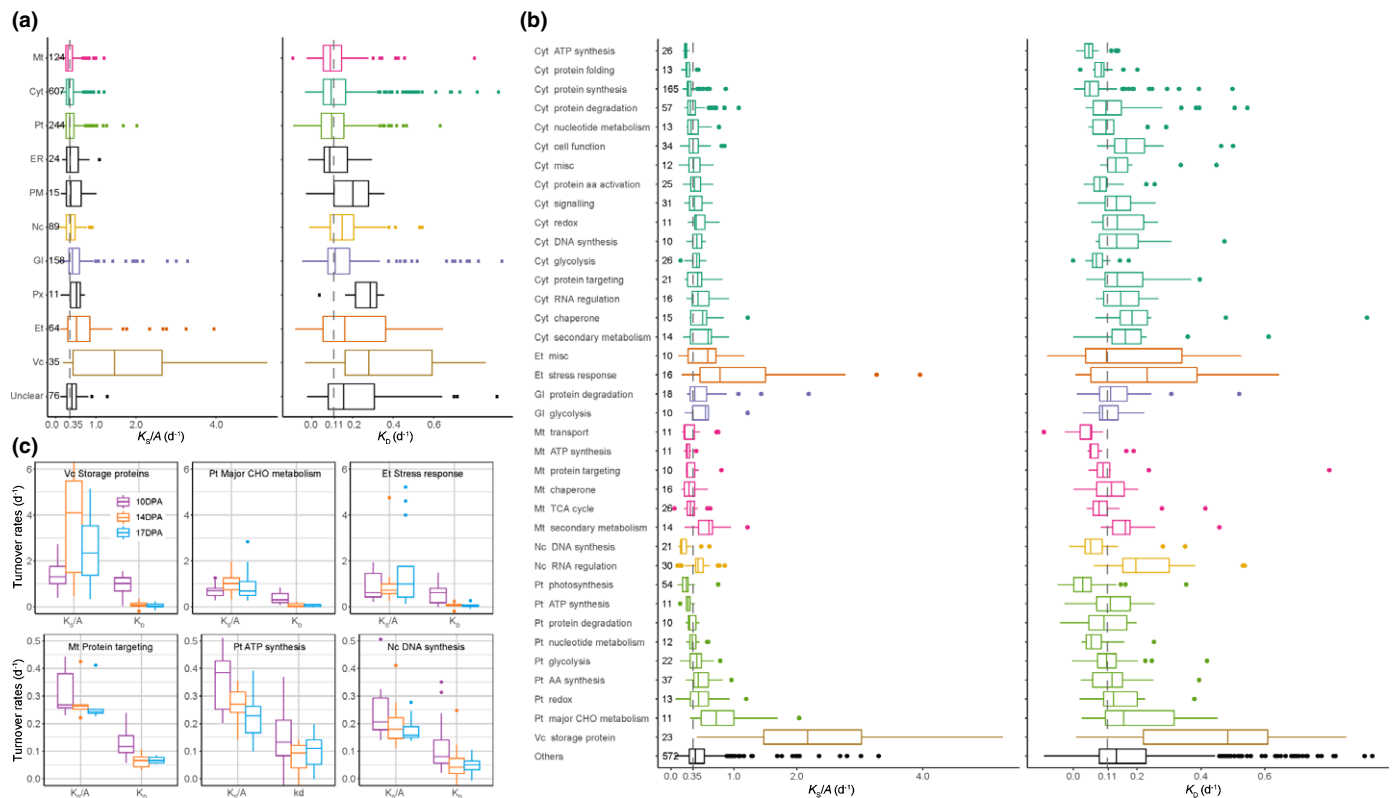
Fig. 3 Rates of synthesis and degradation of 1447 wheat grain proteins during grain development. (a) The averaged protein synthesis (K_S/A) and degradation (K_D) rates calculated across all three time points grouped by the subcellular location of each protein (https://crop-pal.org). The major subcellular locations highlighted are mitochondria (Mt, pink), cytosol (Cyt, green), plastid (Pt, lawngreen), nucleus (Nc, gold), Golgi apparatus (Gl, purple), extracellular (Et, orange-red), and vacuole (Vc, peru). Dashed lines indicate the overall median K_S/A and K_D across all proteins. The number of proteins in each subcellular location is displayed next to the y-axis. Boxes are sorted by increasing order of median K_S/A. (b) The averaged protein synthesis and degradation rates calculated across the three time points grouped by both subcellular location and functional category. Only major functional categories with protein number ≥ 10 were displayed, and minor categories with protein number < 10 were grouped into 'Others'. The colour scheme was the same used in (a). (c) Examples of six functional categories of interest showing the largest difference (upper panel) and smallest difference (lower panel) between K_S/A and K_D at each time point. Thick bars in the boxes indicate median values, box limits are upper and lower quartiles, whiskers represent 1.5 interquartile ranges, and dots represent outliers. Detailed statistical analysis is explained, and relevant results are listed in Supporting Information Table S5.

proteins involved in stress response and proteins involved in protein degradation (Fig. S7b–d).

Protein turnover rates explain varying abundance of proteins in different parts of the grain

To find connections between protein turnover rates and the spatiotemporal abundance patterns of grain proteins, we separately quantified the abundance of 5550 grain protein groups in endosperm, embryo and pericarp (Fig. S8; Table S6). These proteins were then assigned into seven categories based on their protein abundance profile using the definition and equations explained in the Materials and Methods section. Forty percent of these proteins were found evenly balanced in their abundance across grain tissues, c. 32% were assigned as tissue-specific proteins (7% for endosperm, and 12.5% for embryo and pericarp, respectively) and c. 29% as tissue-suppressed proteins, that is proteins present two tissues but low in the third (14% for endosperm, and 7.5% for embryo and pericarp, respectively) (Fig. 4a). The endosperm-specific proteins (Fig. 4c) had high fold

changes and increasing net accumulation rate over development, while pericarp-specific proteins (Fig. 4c) had low fold change in abundance and decreasing in net accumulation rate over time. In comparison, embryo-specific proteins had an increasing net accumulation rate over development but very low turnover rates and fold change in abundance values (Fig. 4c). The proteins with tissue-balanced profiles, showed moderate fold changes and net accumulation rates remained stable over development (Fig. 4c). This pattern was also observed to a lesser extent in protein groups suppressed in a specific tissue (Fig. S9).

Adenosine triphosphate energy budget for wheat grain proteome synthesis and maintenance

The ATP energy cost for both synthesis and degradation of 1140 proteins in the wheat grain proteome was calculated through combining intensity based absolute quantification (iBAQ) values (Table S7), protein turnover rates, amino acid length, and the ATP cost per amino acid residue for protein synthesis and protein degradation (Piques *et al.*, 2009; Kaleta *et al.*, 2013; Peth

et al., 2013) (Table S7). This revealed that during grain development, each grain invested 20% of its total ATP production on protein biogenesis and maintenance. The ATP budget for protein synthesis (9.8 µmol per grain d^{-1}) was nearly nine times larger than for protein degradation (1.2 µmol per grain d^{-1}; Fig. 5a).

Grouping the ATP usage data by the subcellular location of each protein allowed us to assess the relative energy cost of maintaining different subcellular structures in the wheat grain. Maintaining the proteins of the vacuole (the destined location of storage proteins) used one-third of the total ATP budget for protein synthesis although this group only contained 24 unique groups of proteins. This was followed by the largest category,

cytosolic proteins (comprising 469 protein groups), that cost *c.* 25% of the ATP, and the plastid and Golgi apparatus each cost *c.* 13% of the ATP used for protein synthesis (Fig. 5b). The cytosol proteome cost 34% of the total ATP for protein degradation, which was nearly twice that of the vacuole (17.8%). Expressing the ATP usage rate as nmol per million protein copies per grain per day (nmol ATP mcopy^{-1} per grain d^{-1}), the vacuole proteome was the most expensive for protein synthesis on a location basis, costing 144 nmol ATP mcopy^{-1} per grain d^{-1}, which was 15 times higher than the lowest cost compartment, the nucleus, at only 9.3 nmol ATP mcopy^{-1} per grain d^{-1}. Peroxisomes topped the list of protein degradation energy costs, consuming 12 nmol
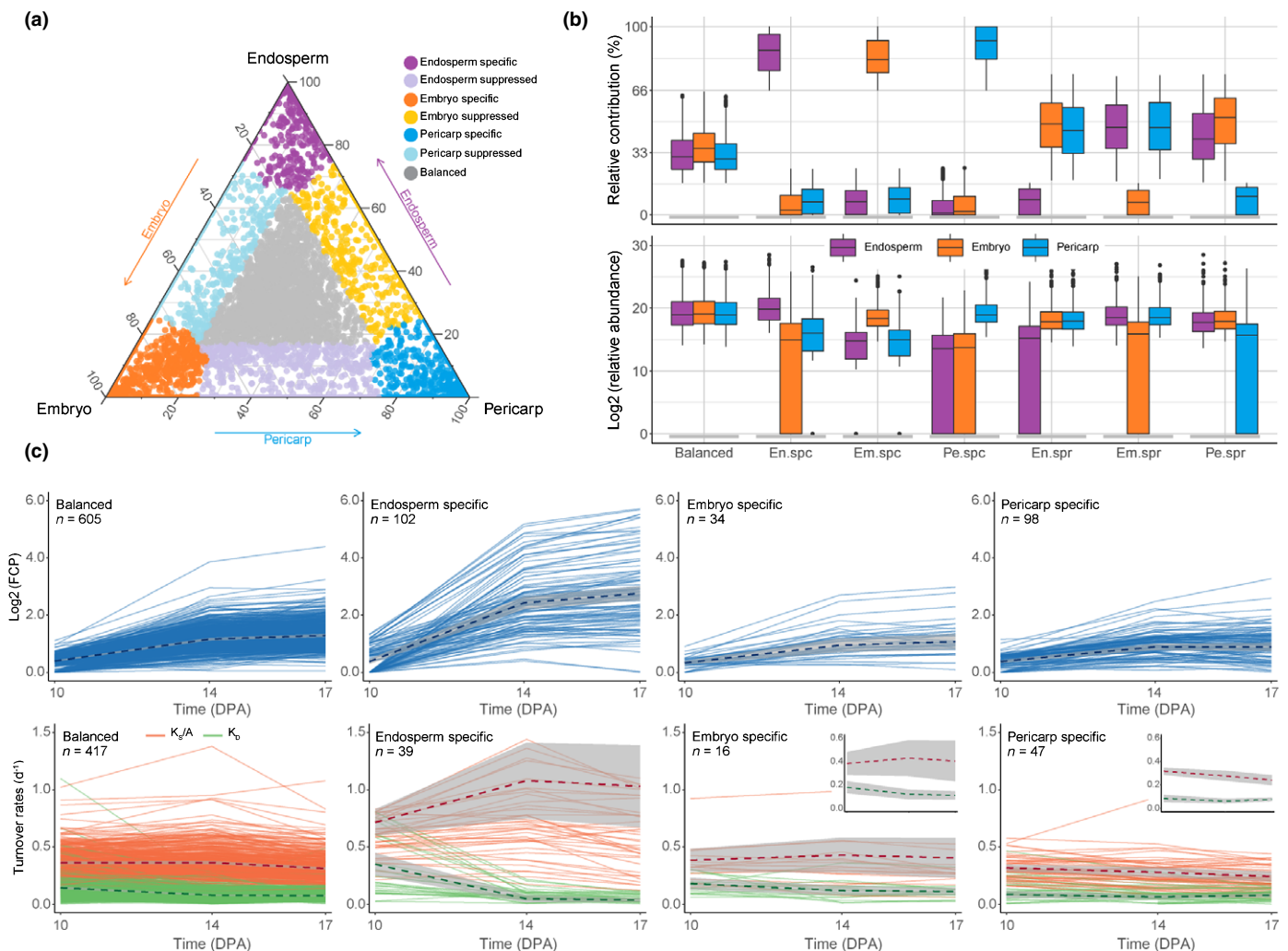

Fig. 4 Changes in protein abundance and protein synthesis and degradation rate profiles of proteins expressed in different wheat grain tissue types during grain development. (a) A ternary plot of the abundances of 5550 protein groups measured in endosperm, embryo and pericarp extracts from grain. Each circle represents a protein and its position indicates the relative contribution of each protein to grain tissue in grain protein abundance. Proteins with a relative contribution ≥ 66% in one tissue and a protein concentration ≥ 3-fold that in the other two tissues are defined as tissue-specific proteins (shown close to triangle vertices), proteins with a relative contribution ≤ 17% in one tissue are defined as tissue-suppressed proteins (between vertices and close to edges), while the remaining proteins are found relatively evenly balanced across grain tissues (grey circles in the middle). (b) Box plots of the relative protein contribution (upper panel) and actual relative abundance estimated via label free quantification (lower panel) for each tissue in each protein expression category. Thick horizonal bars in the boxes indicate median values, box limits are upper and lower quartiles, whiskers represent 1.5 interquartile ranges, and dots represent outliers. (c) Line plots showing fold changes in protein abundance (FCP, blue), protein synthesis rate (orange) and protein degradation rate (green) of balanced and tissue specific protein sets during grain development. Only proteins having values (FCP or turnover rates) at all three time points are included. The dashed line demonstrates the mean values, and the grey shade area shows the 95% confidence intervals. The optimized *y*-axis scale version are inserted for embryo and pericarp specific proteins to highlight the change pattern.

ATP mcopy^{-1} per grain d^{-1}, while the cytosol, by contrast, only consumed 2.2 nmol ATP mcopy^{-1} per grain d^{-1} for this purpose.

When the data was grouped by functional category, we observed that storage proteins and enzymes of major CHO metabolism were the most costly in terms of both protein synthesis and degradation, together they used half the energy budget of

total protein synthesis and a quarter of the total energy budget for protein degradation (Fig. 5c). Storage proteins were the most expensive functional category in terms of synthesis and maintenance of proteins, costing 152 nmol ATP mcopy^{-1} per grain d^{-1} for synthesis and additional 9 nmol ATP mcopy^{-1} per grain d^{-1} for degradation. Less costly protein synthesis and maintenance
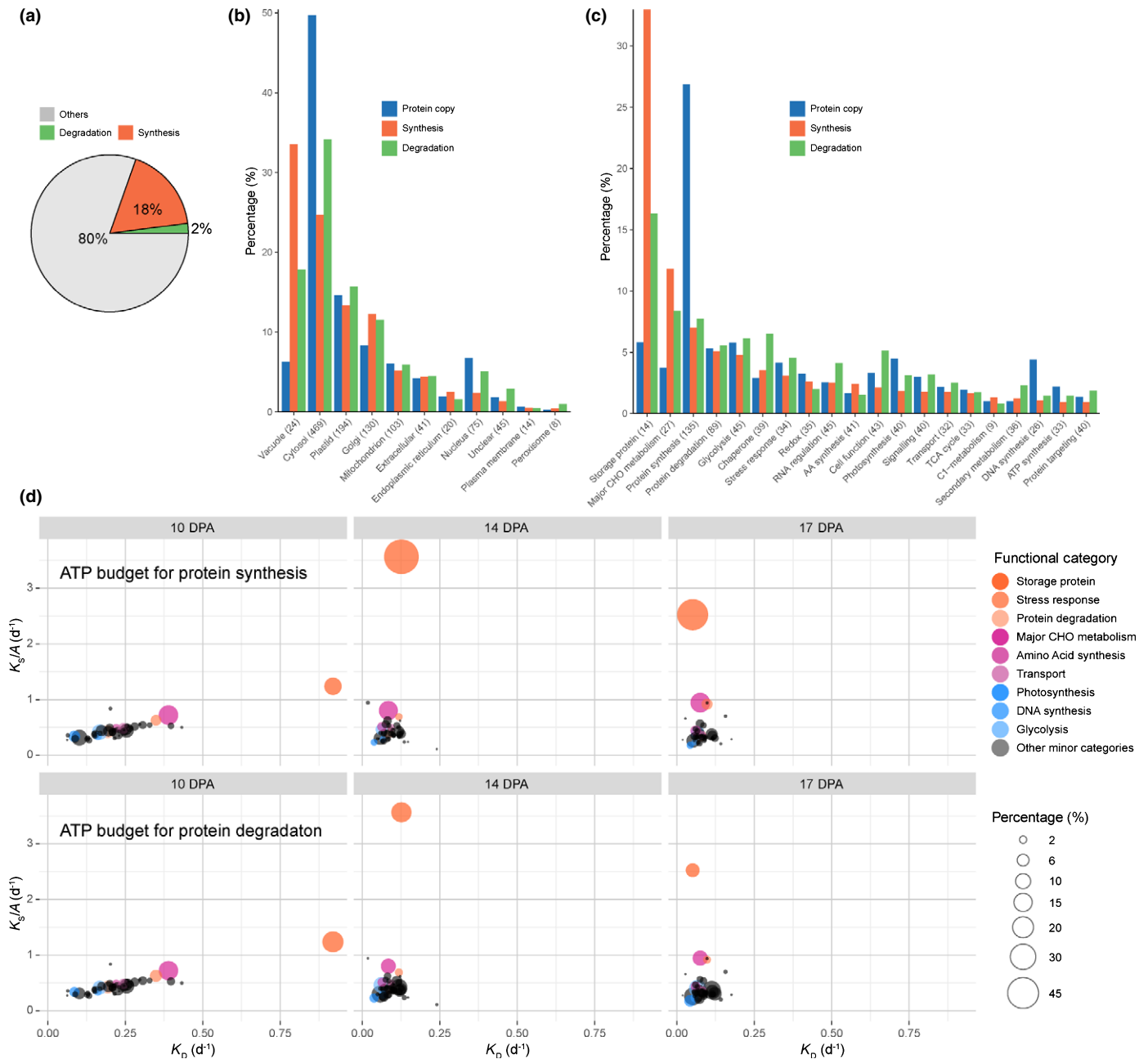

Fig. 5 Adenosine triphosphate (ATP) energy budget used in wheat grain proteome synthesis and maintenance during grain development. (a) The overall proportion of cellular ATP budget used for protein synthesis, protein degradation, and other cell events and maintenance. (b) Proportional distributions of protein copy numbers (intensity based absolute quantification (iBAQ)) and ATP cost of protein building and maintenance of major cellular organelles and subcellular structures. Proteins in location groups sorted by decreasing ATP usage for protein synthesis. The number of proteins in each category is included within brackets. (c) Proportional distributions of protein copy numbers (iBAQ) and ATP cost of protein building and maintenance of protein in major functional categories. (d) Bubble plots showing, by the size of circles, the changing profiles of cellular ATP energy budget for different classes of proteins during grain development. The top three functional categories having both fast K_S/A and K_D rates (orange-red), fast K_S/A and slow K_D rates (violet-red), and both slow K_S/A and K_D rates (blue) are highlighted. Calculations are based on grain total ATP production in (a), but based on total ATP energy budget for protein synthesis or degradation in (b–d).

expense was evident for ribosomal proteins (7 nmol ATP mcopy^{-1} per grain d^{-1} for synthesis and 0.9 nmol ATP mcopy^{-1} per grain d^{-1} for degradation). As expected, the 20 highest cost proteins were predominately storage proteins and major CHO metabolism proteins, among which the highest energy cost for an individual protein was an 11S globulin (TraesCS1A01 G066100.1) that cost nearly 2% of grain ATP in its production during this stage of grain development (Table S7).

Collectively, storage proteins dominated the wheat grain proteome in terms of abundance, fold change in protein, protein turnover rates and ATP energy usage; but this prominence builds over time. The grain invested only 10% of its total ATP energy budget for protein synthesis on the formation of storage proteins at the early grain filling stage (10 DPA), but this subsequently grew 4.5 times in the next 4 d, reaching 45% of the total ATP budget for protein synthesis by 14 DPA, and settled at 36% by 17 DPA (Fig. 5d). The ATP energy budget for degradation of storage proteins showed a similar pattern, increasing at the early stage of grain filling and decreasing at later stages, although it remained at a relatively high level over time. The machinery of major CHO metabolism, which is needed for starch synthesis, showed a rather stable energy usage over time compared to storage proteins. Likewise, proteins in functional categories such as photosynthesis, DNA synthesis and glycolysis showed a relatively stable energy usage over time and only consumed a minor proportion of ATP production in the grain (Fig. 5d).

Wheat storage proteins accumulation during grain filling

To illustrate the complexity of accumulation patterns of members of the seven key storage protein families and their causes from 7 DPA to 17 DPA we integrated six different measures into a single radar graphic (Fig. 6a,b). Our findings indicated that except for globulin 1 encoding genes which peaked at 30 DPA, the messenger RNA (mRNA) of key storage proteins were most abundant at the early grain filling stage and were temporally offset from protein accumulation. A common pattern in synthesis rates and biogenesis energy cost (CostSyn) was shared between storage protein families; they reached the highest level at 14 DPA and remained at this level until at least 17 DPA. In comparison, significantly higher degradation rates and energy consumption were measured at the pre-grain filling stage (10 DPA) than the grain filling stage (from 14 DPA). Collectively these features resulted in a rapid accumulation in storage protein abundance, which increased over 20-fold on average and up to 90-fold for some storage protein isoforms from 10 DPA to 17 DPA (Fig. 6b,c).

Discussion

In this study, we provide an extensive and quantitative understanding of how different wheat grain proteins accumulate during grain development. The resulting protein turnover data allows the costs of individual proteins, protein functional groups, and cell structures during grain development to be calculated, providing an innovative foundation for grain protein engineering strategies.

Previous studies calculated a lag time of 8 h for ^{15}N labelling of proteins in hydroponically growth barley leaves (Nelson *et al.*, 2014a) and 5 h in Arabidopsis young leaves (Li *et al.*, 2017), but the lag involved in long-distance transport from roots to the wheat spike is likely to be considerably longer (Fischer *et al.*, 1998). Furthermore, most protein turnover studies in plants to date have assessed steady-state scenarios where there is little or no developmental change in protein composition (Yang *et al.*, 2010; Nelson *et al.*, 2014a; Li *et al.*, 2017), which is not the case in grain filling. We solved these two problems by experimentally calculating a 28 h lag time for ^{15}N incorporation (Fig. S3) and measuring the fold change in abundance for each protein of interest during grain development using a spike-in of a fully ^{15}N labelled proteome (Figs 2, S6). This has allowed not only the protein turnover rates of over a thousand proteins to be determined, but to do so in a background of proteins changing in relative abundance over a 0.018-fold to 126-fold range.

As autotrophs, plants have access to a large source of ATP via photosynthesis in source leaves. However, the ATP yielded by this process is largely invested in sucrose synthesis that is transported to sink tissues, which leaves oxidative phosphorylation by respiration as the primary source for cytosolic ATP-dependent processes like protein synthesis and degradation (Flugge *et al.*, 2011; Li *et al.*, 2017). Based on this we calculated the proportional energy cost for synthesis and degradation of the wheat grain proteome during grain filling based on grain respiration rates (Fig. 5). Our data show that approximately 20% of total grain ATP production through respiration is used for grain proteome biogenesis and maintenance, and nearly half of this budget is invested exclusively in storage protein synthesis. This proportion was similar in size to reports of the cost of Arabidopsis leaf protein turnover which varied from 16% to 42% of total ATP depending on the age of the examined leaf (Li *et al.*, 2017). However, in grains this ATP investment is co-commitment with the high ATP demand of starch synthesis at the same times during development (Keeling *et al.*, 1988; Jenner *et al.*, 1991). Collectively, ATP provision to protein synthesis and degradation and the starch synthesis represent an energy constraint that will dictate the relative investment in starch and protein in the final grain.

Dough rheological properties and bread-making quality in wheat are primarily determined by gluten quantity (Delcour *et al.*, 2012). In our development analysis, four storage protein families that are key components of gluten polymers, namely HMW-GS, LMW-GS, gliadin-like avenin and gamma-gliadin, represent 85% of storage protein abundance (Fig. 6c; Table S8); consistent with previous studies reporting 80–90% of total grain protein is gluten polymers (Shewry, 2009; Zorb *et al.*, 2018). Extensive previous studies have also demonstrated that gluten quality, both the ratio of gliadin : glutenin and the ratio of HMW-GS : LMW-GS, strongly influences dough viscosity and elasticity, thus governing bread-making quality traits (Barak *et al.*, 2014; Dhaka & Khatkar, 2015; Geisslitz *et al.*, 2019). The ratio of HMW-GS : LMW-GS is typically *c.* 0.67 in mature grains (Zorb *et al.*, 2018), our data show HMW-GS : LMW-GS continuously decreased overtime from 3.66 at 10 DPA to 1.63
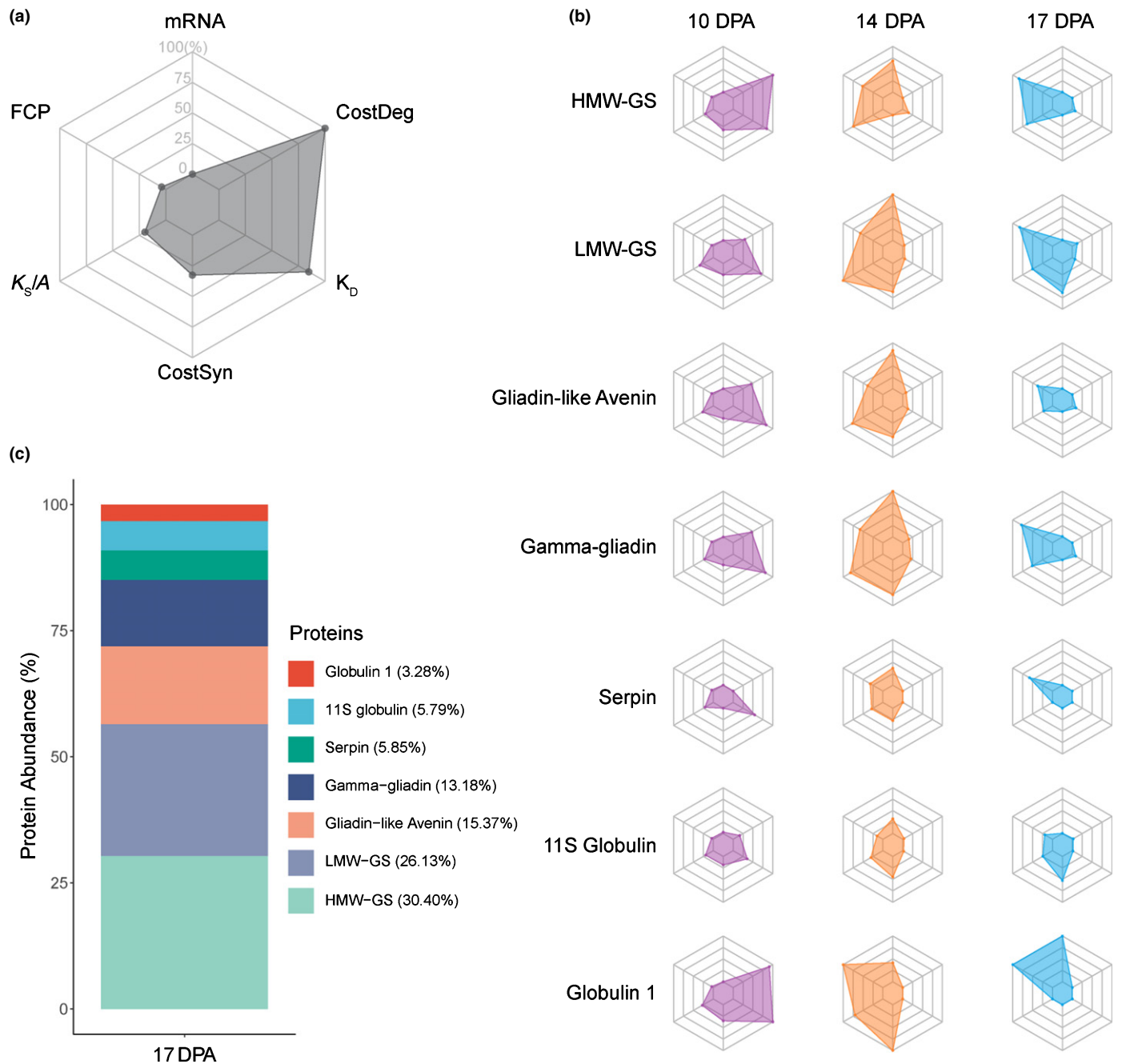
Fig. 6 Accumulation profiles of key storage protein families during grain filling. (a) The example radar chart. Six categories of data were collected and analysed, namely transcript data (messenger RNA (mRNA), rang: 0–1000 tpm), fold changes in protein abundance (FCP, range: 1–25 folds), protein synthesis rate (K_S/A, range: 0–5.84 d^{-1}), ATP energy cost for protein synthesis (CostSyn, range: 0–290.2 nmol ATP mcopy^{-1} per grain d^{-1}), protein degradation rate (K_D, range: 0–1.36 d^{-1}), and ATP energy cost for protein degradation (CostDeg, range: 0–51.6 nmol ATP mcopy^{-1} per grain d^{-1}). mRNA $\geq$ 1000 tpm and FCP $\geq$ 25-fold were treated as 100%, while missing values were replaced by zero for visualization. The percentage normalization was conducted across all proteins and time points allows comparisons to be made in time series and between protein types. The raw data and statistical test results are collected at Supporting Information Table S8. (b) Radar charts showing the six molecular profiles of the key wheat grain storage proteins at 10, 14, and 17 d post-anthesis (DPA) during grain filling. (c) Abundance of the key wheat grain storage proteins at 17 DPA.

by 14 DPA and ending up 1.16 by 17 DPA. Unlike the ratio of HMW-GS : LMW-GS, the ratio of gliadin : glutenin remained stable during grain development in our hands (Table S8). Protein turnover data reveals that 25% of these newly synthesized storage proteins appear to be turning over during grain development rather than being stored and that instability of storage proteins

was most prominent early in grain development between 10 and 17 DPA. Wheat storage proteins are generally assembled, folded and aggregated in the ER, followed by a trafficking event mediated by protein bodies to vacuoles for storage through either a Golgi–vacuole route or the ER–vacuole route (Tosi *et al.*, 2009; Pedrazzini *et al.*, 2016). Previous evidence has suggested that

storage proteins are stabilized during the processing within the ER due to the formation of complex polymers through disulphide and noncovalent bonds (inter- and/or intra-chain bonds) (Galili *et al.*, 1995; Tosi *et al.*, 2009). Dominguez & Cejudo (1996) showed that extractable wheat grain endoprotease activity reached its maximum at 15 DPA and then decreased afterwards. Likewise, Nadaud *et al.* (2010) showed grain proteolysis activity peaked at approximately 10 DPA, and showed a decrease pattern over the following 4 d. Our data also indicate a significant decrease in protein degradation machinery of the endomembrane system from 10 DPA to 17 DPA (Table S7). These high degradation rates of storage proteins detected at 10 DPA are not the case for all storage protein isoforms (Fig. 6b; Table S7), providing a breeding or biotechnological pathway to select for lower cost storage proteins with lower degradation rates. For example, specific sequences or protein domains of targeted storage proteins could be changed to increase their stability, or genes deleted to avoid protein cycling, or more stable storage proteins overexpressed or genes duplicated. Alternatively, our knowledge of the timing of storage protein turnover earlier in grain filling can focus efforts on the ER-localized proteolytic machinery operating at this time and minimizing its contribution to protein cycling. Modifying the stability of one or more storage proteins may impact the expression of other grain proteins, provide more ATP for other processes or retain respiratory substrates for other purposes. Whether such changes will negatively or positively impact other grain traits remains to be determined from further studies.

Extensive effort has been placed into assessing the correlation between transcript level and protein abundance, however only *c.* 40% of the variation in protein abundance is typically explained by transcript data in eukaryotes, including plants (Abreu *et al.*, 2009; McLoughlin *et al.*, 2018; Reich *et al.*, 2020; Zander *et al.*, 2020). In wheat there is only a 32% concordance between protein and transcript expression profiles observed during grain development (Tahir *et al.*, 2020). This atlas of wheat grain protein turnover rates contributes to explaining the remaining variation in protein abundance not correlated to transcript levels. As an atlas it shows that despite variation of turnover rate for different proteins approaching 100 fold, protein turnover rates are highly correlated with their changing profiles of FCP over time when a net accumulation rate calculation is considered as the key driver of protein abundance alterations (Figs 3, S10). It is also known that spatiotemporal regulatory mechanisms broadly exist in live-systems and play essential roles in protein abundance regulation to meet various biological scenarios (Brady *et al.*, 2007; Pfeifer *et al.*, 2014; Li *et al.*, 2017; Selkrig *et al.*, 2020). This pattern is also evident in our wheat grain data and we show that the higher turnover rates of storage proteins when compared to other protein groups drives the preferential accumulation of storage proteins as one of the largest cellular events during grain filling (Figs 2–4).

Overall this study provides a comprehensive and in-depth view of which key storage proteins accumulation during pre- and the early-mid grain filling stage. In addition, the quantitative data for nonstorage proteins provides insights into a wide range of biological events during wheat grain development, such as the protein machinery for starch accumulation and the initiation of desiccation stress responses. Future studies will be needed to reveal why wheat grains partake in cycles of protein synthesis and degradation and find approaches to alter this cycling such as knockout of unstable storage proteins and expression of more stable versions using either conventional cross breeding approaches or gene editing technologies. Success in this pursuit could help increase grain protein content, improve energy use efficiency of protein production, and help meet the unprecedented food demand for sustainable plant-based protein production in modern agriculture.

Author contributions

HC, OD and AHM conceived and designed the project. HC and OD performed the experiment and data analysis. HC wrote the manuscript, AHM and OD read and corrected the manuscript.

ORCID

Hui Cao https://orcid.org/0000-0002-1062-9043
Owen Duncan https://orcid.org/0000-0001-6999-1509
A. Harvey Millar https://orcid.org/0000-0001-9679-1473

Data availability

The primary MS data files are available via ProteomeXchange with identifier PXD022231.

References

Abreu RD, Penalva LO, Marcotte EM, Vogel C. 2009. Global signatures of protein and mRNA expression levels. *Molecular BioSystems* 5: 1512–1526.

Barak S, Mudgil D, Khatkar BS. 2014. Influence of gliadin and glutenin fractions on rheological, pasting, and textural properties of dough. *International Journal of Food Properties* 17: 1428–1438.

Blum A, Mayer J, Golan G. 1983. Chemical desiccation of wheat plants as a simulator of post-anthesis stress. 2. Relations to drought stress. *Field Crops Research* 6: 149–155.

Borrill P, Ramirez-Gonzalez R, Uauy C. 2016. expVIP: a customizable RNA-seq data analysis and visualization platform. *Plant Physiology* 170: 2172–2186.

Brady SM, Orlando DA, Lee JY, Wang JY, Koch J, Dinneny JR, Mace D, Ohler U, Benfey PN. 2007. A high-resolution root spatiotemporal map reveals dominant expression patterns. *Science* 318: 801–806.

Cao H, He M, Zhu C, Yuan LL, Dong LW, Bian YW, Zhang WY, Yan YM. 2016. Distinct metabolic changes between wheat embryo and endosperm during grain development revealed by 2D-DIGE-based integrative proteome analysis. *Proteomics* 16: 1515–1536.

Dawson TE, Mambelli S, Plamboeck AH, Templer PH, Tu KP. 2002. Stable isotopes in plant ecology. *Annual Review of Ecology and Systematics* 33: 507–559.

Delcour JA, Joye IJ, Pareyt B, Wilderjans E, Brijs K, Lagrain B. 2012. Wheat gluten functionality as a quality determinant in cereal-based food products. *Annual Review of Food Science and Technology* 3: 469–492.

Dhaka V, Khatkar BS. 2015. Effects of gliadin/glutenin and HMW-GS/LMW-GS ratio on dough rheological properties and bread-making potential of wheat varieties. *Journal of Food Quality* 38: 71–82.

Dominguez F, Cejudo FJ. 1996. Characterization of the endoproteases appearing during wheat grain development. *Plant Physiology* 112: 1211–1217.

Duncan O, Trosch J, Fenske R, Taylor NL, Millar AH. 2017. Resource: mapping the *Triticum aestivum* proteome. *The Plant Journal* 89: 601–616.

Fan KT, Rendahl AK, Chen WP, Freund DM, Gray WM, Cohen JD, Hegeman AD. 2016. Proteome scale-protein turnover analysis using high resolution mass spectrometric data from stable-isotope labeled plants. *Journal of Proteome Research* 15: 851–867.

Fischer WN, Andre B, Rentsch D, Krolkiewicz S, Tegeder M, Breitkreuz K, Frommer WB. 1998. Amino acid transport in plants. *Trends in Plant Science* 3: 188–195.

Flugge UI, Hausler RE, Ludewig F, Gierth M. 2011. The role of transporters in supplying energy to plant plastids. *Journal of Experimental Botany* 62: 2381–2392.

Foley JA, Ramankutty N, Brauman KA, Cassidy ES, Gerber JS, Johnston M, Mueller ND, O'Connell C, Ray DK, West PC *et al.* 2011. Solutions for a cultivated planet. *Nature* 478: 337–342.

Galili G, Altschuler Y, Levanony H, Giorinisilfen S, Shimoni Y, Shani N, Karchi H. 1995. Assembly and transport of wheat storage proteins. *Journal of Plant Physiology* 145: 626–631.

Galland M, Huguet R, Arc E, Cueff G, Job D, Rajjou L. 2014. Dynamic proteomics emphasizes the importance of selective mRNA translation and protein turnover during Arabidopsis seed germination. *Molecular & Cellular Proteomics* 13: 252–268.

Geisslitz S, Longin CFH, Scherf KA, Koehler P. 2019. Comparative study on gluten protein composition of ancient (Einkorn, Emmer and Spelt) and modern wheat species (durum and common wheat). *Foods* 8: 409.

Herman EM, Larkins BA. 1999. Protein storage bodies and vacuoles. *Plant Cell* 11: 601–613.

Hooper CM, Castleden IR, Aryamanesh N, Jacoby RP, Millar AH. 2016. Finding the subcellular location of barley, wheat, rice and maize proteins: the compendium of crop proteins with annotated locations (cropPAL). *Plant and Cell Physiology* 57: e9.

Jenner CF, Ugalde TD, Aspinall D. 1991. The physiology of starch and protein deposition in the endosperm of wheat. *Australian Journal of Plant Physiology* 18: 211–226.

Kaleta C, Schauble S, Rinas U, Schuster S. 2013. Metabolic costs of amino acid and protein production in *Escherichia coli*. *Biotechnology Journal* 8: 1105–1114.

Keeling PL, Wood JR, Tyson RH, Bridges IG. 1988. Starch biosynthesis in developing wheat-grain – evidence against the direct involvement of triose phosphates in the metabolic pathway. *Plant Physiology* 87: 311–319.

Li L, Nelson CJ, Trosch J, Castleden I, Huang SB, Millar AH. 2017. Protein degradation rate in *Arabidopsis thaliana* leaf growth and development. *Plant Cell* 29: 207–228.

Lyon D, Castillejo MA, Mehmeti-Tershani V, Staudinger C, Kleemaier C, Wienkoop S. 2016. Drought and recovery: independently regulated processes highlighting the importance of protein turnover dynamics and translational regulation in *Medicago truncatula*. *Molecular & Cellular Proteomics* 15: 1921–1937.

Martin SF, Munagapati VS, Salvo-Chirnside E, Kerr LE, Le Bihan T. 2012. Proteome turnover in the green alga *Ostreococcus tauri* by time course 15N metabolic labeling mass spectrometry. *Journal of Proteome Research* 11: 476–486.

McLoughlin F, Augustine RC, Marshall RS, Li FQ, Kirkpatrick LD, Otegui MS, Vierstra RD. 2018. Maize multi-omics reveal roles for autophagic recycling in proteome remodelling and lipid turnover. *Nature Plants* 4: 1056–1070.

Munns R, James RA. 2003. Screening methods for salinity tolerance: a case study with tetraploid wheat. *Plant and Soil* 253: 201–218.

Muqaddasi QH, Brassac J, Ebmeyer E, Kollers S, Korzun V, Argillier O, Stiewe G, Plieske J, Ganal MW, Roder MS. 2020. Prospects of GWAS and predictive breeding for European winter wheat's grain protein content, grain starch content, and grain hardness. *Scientific Reports* 10: 12541.

Nadaud I, Girousse C, Debiton C, Chambon C, Bouzidi MF, Martre P, Branlard G. 2010. Proteomic and morphological analysis of early stages of wheat grain development. *Proteomics* 10: 2901–2910.

Nelson CJ, Alexova R, Jacoby RP, Millar AH. 2014a. Proteins with high turnover rate in barley leaves estimated by proteome analysis combined with in planta isotope labeling. *Plant Physiology* 166: 91–108.

Nelson CJ, Li L, Jacoby RP, Millar AH. 2013. Degradation rate of mitochondrial proteins in *Arabidopsis thaliana* cells. *Journal of Proteome Research* 12: 3449–3459.

Nelson CJ, Li L, Millar AH. 2014b. Quantitative analysis of protein turnover in plants. *Proteomics* 14: 579–592.

Nelson CJ, Millar AH. 2015. Protein turnover in plant biology. *Nature Plants* 1: 15017.

O'Leary BM, Lee CP, Atkin OK, Cheng R, Brown TB, Millar AH. 2017. Variation in leaf respiration rates at night correlates with carbohydrate and amino acid supply. *Plant Physiology* 174: 2261–2273.

Pedrazzini E, Mainieri D, Marrano CA, Vitale A. 2016. Where do protein bodies of cereal seeds come from? *Frontiers in Plant Science* 7: 1139.

Peth A, Nathan JA, Goldberg AL. 2013. The ATP costs and time required to degrade ubiquitinated proteins by the 26S proteasome. *Journal of Biological Chemistry* 288: 29215–29222.

Pfeifer M, Kugler KG, Sandve SR, Zhan B, Rudi H, Hvidsten TR, Mayer KFX, Olsen O-A. 2014. Genome interplay in the grain transcriptome of hexaploid bread wheat. *Science* 345: 1250091.

Piques M, Schulze WX, Hohne M, Usadel B, Gibon Y, Rohwer J, Stitt M. 2009. Ribosome and transcript copy numbers, polysome occupancy and enzyme dynamics in Arabidopsis. *Molecular Systems Biology* 5: 314.

Ramírez-González RH, Borrill P, Lang D, Harrington SA, Brinton J, Venturini L, Davey M, Jacobs J, van Ex F, Pasha A *et al.* 2018. The transcriptional landscape of polyploid wheat. *Science* 361: eaar6089.

Rangan P, Furtado A, Henry RJ. 2017. The transcriptome of the developing grain: a resource for understanding seed development and the molecular control of the functional and nutritional properties of wheat. *BMC Genomics* 18: 766.

Reich S, Nguyen CDL, Has C, Steltgens S, Soni H, Coman C, Freyberg M, Bichler A, Seifert N, Conrad D *et al.* 2020. A multi-omics analysis reveals the unfolded protein response regulon and stress-induced resistance to folate-based antimetabolites. *Nature Communications* 11: 2936.

Rogers SO, Quatrano RS. 1983. Morphological staging of wheat caryopsis development. *American Journal of Botany* 70: 308–311.

Scafaro AP, Negrini ACA, O'Leary B, Rashid FAA, Hayes L, Fan Y, Zhang Y, Chochois V, Badger MR, Millar AH *et al.* 2017. The combination of gas-phase fluorophore technology and automation to enable high-throughput analysis of plant respiration. *Plant Methods* 13: 16.

Schaffner W, Weissmann C. 1973. A rapid, sensitive, and specific method for the determination of protein in dilute solution. *Analytical Biochemistry* 56: 502–514.

Selkrig J, Li N, Hausmann A, Mangan MSJ, Zietek M, Mateus A, Bobonis J, Sueki A, Imamura H, El Debs B *et al.* 2020. Spatiotemporal proteomics uncovers cathepsin-dependent macrophage cell death during Salmonella infection. *Nature Microbiology* 5: 1119–1133.

Shewry PR. 2009. Wheat. *Journal of Experimental Botany* 60: 1537–1553.

Shewry PR, Hey SJ. 2015. The contribution of wheat to human diet and health. *Food and Energy Security* 4: 178–202.

Tahir A, Kang J, Choulet F, Ravel C, Romeuf I, Rasouli F, Nosheen A, Branland G. 2020. Deciphering carbohydrate metabolism during wheat grain development via integrated transcriptome and proteome dynamics. *Molecular Biology Reports* 47: 5439–5449.

Thimm O, Blasing O, Gibon Y, Nagel A, Meyer S, Kruger P, Selbig J, Muller LA, Rhee SY, Stitt M. 2004. MAPMAN: a user-driven tool to display genomics data sets onto diagrams of metabolic pathways and other biological processes. *The Plant Journal* 37: 914–939.

Tilman D, Cassman KG, Matson PA, Naylor R, Polasky S. 2002. Agricultural sustainability and intensive production practices. *Nature* 418: 671–677.

Tosi P, Parker M, Gritsch CS, Carzaniga R, Martin B, Shewry PR. 2009. Trafficking of storage proteins in developing grain of wheat. *Journal of Experimental Botany* 60: 979–991.

Voss-Fels KP, Stahl A, Wittkop B, Lichthardt C, Nagler S, Rose T, Chen T-W, Zetzsche H, Seddig S, Majid Baig M *et al.* 2019. Breeding improves wheat productivity under contrasting agrochemical input levels. *Nature Plants* 5: 706–714.

Wang Y, Yang F, Gritsenko MA, Wang Y, Clauss T, Liu T, Shen Y, Monroe ME, Lopez-Ferrer D, Reno T *et al.* 2011. Reversed-phase chromatography with multiple fraction concatenation strategy for proteome profiling of human MCF10A cells. *Proteomics* 11: 2019–2026.

Wessel D, Flugge UI. 1984. A method for the quantitative recovery of protein in dilute-solution in the presence of detergents and lipids. *Analytical Biochemistry* 138: 141–143.

Yang XY, Chen WP, Rendahl AK, Hegeman AD, Gray WM, Cohen JD. 2010. Measuring the turnover rates of Arabidopsis proteins using deuterium oxide: an auxin signaling case study. *The Plant Journal* 63: 680–695.

Yao SX, Zhang Y, Chen YL, Deng HT, Liu JY. 2014. SILARS: an effective stable isotope labeling with ammonium nitrate-15N in rice seedlings for quantitative proteomic analysis. *Molecular Plant* 7: 1697–1700.

Zander M, Lewsey MG, Clark NM, Yin L, Bartlett A, Saldierna Guzmán JP, Hann E, Langford AE, Jow B, Wise A *et al.* 2020. Integrated multi-omics framework of the plant response to jasmonic acid. *Nature Plants* 6: 290–302.

Zorb C, Ludewig U, Hawkesford MJ. 2018. Perspective on wheat yield and quality with reduced nitrogen supply. *Trends in Plant Science* 23: 1029–1037.

Supporting Information

Additional Supporting Information may be found online in the Supporting Information section at the end of the article.

Fig. S1 Optimization of *in vivo* grain protein labelling approach during grain development.

Fig. S2 A flow diagram of experiment design, sample preparation, mass spectrometry data acquisition and analysis.

Fig. S3 The time lag of label incorporation into wheat grain proteins.

Fig. S4 Mass spectrum images of amino acids and peptides over a 30-h time course to estimate labelling lag time.

Fig. S5 Data quality verification of spike-in and progressive labelling data.

Fig. S6 The individual fold changes in protein abundance of wheat grain proteins at 10 and 14 DPA summarized by their functional categories.

Fig. S7 Relatively slow and fast turning over wheat grain proteins during grain development.

Fig. S8 Data quality verification of wheat grain tissue data sets.

Fig. S9 Changes in fold changes in protein abundance and turnover rate profiles of proteins present in a lower abundance in a given tissue type during grain development.

Fig. S10 Changes in turnover rates of proteins with high and low fold changes in protein abundance during grain development.

Methods S1 Liquid chromatography–mass spectrometry data processing to generate fold changes in protein abundance, labelled protein fraction, protein turnover and adenosine triphosphate costs.

Table S1 Full data list of grain fresh weight, grain respiration rate and total grain adenosine triphosphate production.

Table S2 Full data list of lag time modelling, gas chromatography–tandem mass spectrometry data and liquid chromatography–tandem mass spectrometry data.

Table S3 Full data list used for data quality control analysis.

Table S4 Full data list of wheat grain individual fold changes in protein abundance values during grain development.

Table S5 Full data list of wheat grain protein turnover rates during grain development.

Table S6 Full data list of protein relative abundance for embryo, endosperm and pericarp proteomes.

Table S7 Full data list of adenosine triphosphate energy budget used for wheat grain protein turnover during grain development.

Table S8 Full data list of wheat grain key storage proteins accumulation profiles during grain development.

Please note: Wiley Blackwell are not responsible for the content or functionality of any Supporting Information supplied by the authors. Any queries (other than missing material) should be directed to the *New Phytologist* Central Office.